Precision Engineering 37 (2013) 107–116

Contents lists available at SciVerse ScienceDirect

Precision Engineering

journal homepage: www.elsevier.com/locate/precision

Characteristic switching of a multilayer thin electrostatic actuator by a driving signal for an ultra-precision motion stage

Mariam Md Ghazaly, Kaiji Sato*

Interdisciplinary Graduate School of Science and Engineering, Tokyo Institute of Technology, 4259-G2-17 Nagatsuta, Midori-ku, Yokohama 226-8502, Japan

ARTICLE INFO

Article history:
Received 5 February 2012
Received in revised form 9 May 2012
Accepted 17 May 2012
Available online 25 July 2012

Keywords:
Electrostatic actuator
Multilayer
Lubricating oil
Fine-motion stage
PID controller
Positioning
Holding signal
Holding force

ABSTRACT

The present paper describes the characteristic switching of a multilayer thin electrostatic actuator supported by only lubricating oil and its application in the control of an ultra-precision fine stage. Friction forces often deteriorate the response and positioning accuracy of a control system. However, they generate a large holding force, which is needed to precisely maintain the stage position in fine stages. When the lightweight electrode layers in the electrostatic actuator are supported by only lubricating oil, the contact condition between the electrode layers can be changed by the attractive forces resulting from the driving signal, which consequently influences the frictional effect. Thus, suitable driving signals have the potential to adjust the frictional effect for fine motion with a large holding force and a wide and fast motion. In this paper, suitable driving signals for switching between two frictional conditions (i.e., low friction for the wide and fast motion and high friction for the fine motion with a large holding force) are examined and clarified. First, the relationship between the driving signals and the working range of the actuator is explained. Then, the holding force characteristics and the driving signals for switching between the frictional conditions are discussed. Finally, the actuator control system is designed based on the findings. The control system includes a PID compensator and a driving signal unit that generates two driving signals. One driving signal provides a driving mode with a holding force for a working range smaller than 250 nm. The other driving signal provides a wide driving mode for a working range wider than 250 nm under low-friction conditions. The driving signal is determined so as to quickly change the frictional effect. A combination of these modes (referred to as the dual driving mode) is implemented in the actual multilayer electrostatic actuator, and its effectiveness is validated experimentally. The actuator exhibits a positioning error of less than 14 nm with a continuous holding force of 0.205 N.

1. Introduction

Precise point-to-point (PTP) positioning is crucial in a fine-motion stage. In microscope systems [1–9], optical systems [10–17], and semiconductor manufacturing systems [18–21], high response and high positioning accuracy are critical. In microscope systems [1,9–16], samples need to be finely positioned and precisely held. In optical systems, mirrors and optical fibers must be aligned, tilted, and held with precision [2–8,22]. In semiconductor manufacturing systems [17–20], substrates are precisely positioned and held using fine stages. As a rule, the fine stages are required to have high positioning accuracy, a short positioning time, a sufficient working range, a simple structure, the ability to generate sufficient force, and low heat. In addition, a holding force for precisely maintaining the position of the object is also required. To satisfy this requirement, the stages often have mechanisms that generate the holding force [22–27]. In [23], a self-locking mechanism with a piezoelectric actuator produces the frictional effect needed to hold the object. In [10,22,24–27], additional holding mechanisms have been implemented to maintain precise positioning. These holding mechanisms (with the aid of holding signals) enable the fine stages to hold and precisely position objects.

To date, numerous types of fine stages have been designed and used. In these fine stages, piezoelectric actuators [22–25], electromagnetic actuators [26–30], and electrostatic actuators [31–36] have been implemented. Although electromagnetic actuators are the most widely used, electrostatic actuators have some advantages in terms of their heat production and material availability compared with electromagnetic actuators. In addition, unlike piezoelectric actuators, electrostatic actuators are able to transmit power without mechanical contact and do not require hinges, which make the systems complex. Previously, various types of electrostatic actuators have been designed which show good performances. Variable-capacitance motors [31–34] and induction motor type electrostatic actuators [35] have been proposed, which

* Corresponding author. Tel.: +81 45 924 5045; fax: +81 45 924 5483.
E-mail addresses: ghazaly.m.aa@m.titech.ac.jp, mariam@utem.edu.my (M. Md Ghazaly), sato.k.ah@m.titech.ac.jp (K. Sato).

0141-6359/$ – see front matter © 2012 Elsevier Inc. All rights reserved.
http://dx.doi.org/10.1016/j.precisioneng.2012.07.005

enable a longer working range of motion that exceeds 200 μm. In these actuators [31,32,35], Higuchi et al. implemented precise beads as rolling elements of a ball guide in order to reduce the friction between electrode layers without groves to guide the beads, and Ghodssi et al. [33,34] used microball bearings with a 3D guide structure fabricated on the mover and stator layers to support the mover. These supporting methods are effective at increasing the advantages of electrostatic actuators. However, they require complex fabrication processes for the guide structure and the mechanism that retains the numerous beads between the mover and stator layers used to maintain the gap.

As a solution, an electrostatic actuator supported by only lubricating oil has been proposed [36]. Its mover has a simpler structure and is cost effective. The electrode layers of the actuator are lightweight enough to maintain the gap and reduce the frictional force between the layers without applying voltage. In the actuator, the motion characteristics depend on the driving signal since the frictional condition is changed by the driving signal. In [36], it is shown that a suitable pulse driving signal provides low friction, a long working range, and high positioning accuracy. However, the pulse driving signal is not suitable for continuously producing the holding force, and it is desired to satisfy both the wide range of motion and the fine and precise motion with a continuous holding force.

Therefore, in this paper, the focus will be on the characteristic switching of the electrostatic actuator supported by only lubricating oil and its application in the control of an ultra-precision fine stage to obtain both a wide range of motion and a fine and precise motion with a continuous holding force. For this, the frictional force exhibited by the electrostatic actuator is used to continuously generate the holding force. A suitable signal for switching the frictional condition is examined, and the effectiveness of the control method with the signal is experimentally validated.

In Section 2, the structure, working principles, and experimental setup of the electrostatic actuator are described. In Section 3, the relationships between the driving signals, the working ranges, and the frictional effect due to the holding signal are discussed to determine a suitable driving signal. In Section 4, a suitable control system is designed based on the driving signals of the actuator, and the control performance is demonstrated. Finally, the conclusions are presented in Section 5.

2. Structure and working principle of the multilayer electrostatic actuator

The electrostatic actuator presented in this paper is a variable-capacitance motor type actuator that has two mover layers [36].

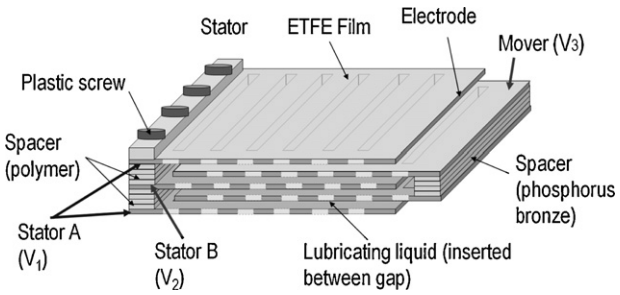

Fig. 1. Schematic diagram of an experimental two-layer electrostatic actuator [36].

Fig. 1 shows a schematic diagram of the experimental two-layer electrostatic actuator. The actuator consists of electrode layers that are alternately stacked together and supported by lubricating oil. The electrodes are covered with ethylene thetrafluoroethylene (ETFE) isolation film to reduce the friction between the electrode layers. To realize bidirectional motion, voltages V_1 and V_2 are applied to Stator A and Stator B, whilst voltage V_3 is set to zero and applied to the mover shown in Fig. 2. Stator A is located so that the electrode beams of Stator A do not face those of Stator B in the z-direction. The working range is equal to the length between the beam centers of Stators A and B in the x-direction. The working range of the experimental actuator is 500 μm. Voltages V_1 and V_2 are out of phase by π. In the range, the applied voltage patterns of Fig. 2(a) and (b) generate the thrust force to the left and the right, respectively. The thrust force is proportional to the square of the applied voltage [36]. Only lubricating oil is used to reduce the friction between the electrode layers (without precise beads) for easy fabrication and maintenance. Silicone oil with a viscosity of 10 mPa s and a dielectric constant of 2.65 is used as the lubricating oil. Fig. 3 shows an overall view of the experimental setup for examining the motion characteristics. The setup includes a digital signal processing system, two high-voltage power amplifiers, and a capacitance displacement sensor. The measurement range of the sensor is 50 μm, and the evaluation range of the actuator is less than 50 μm. Thus, in the present study, the full working range-of-motion characteristics are examined within a range of 40 μm. Table 1 shows the specifications of the electrostatic actuator.

3. Effect of driving signal on actuator characteristics

When the lightweight electrode layers are supported by only lubricating oil, the attractive forces resulting from the driving signal influence the contact condition between the electrode layers (i.e., the frictional effect). Therefore, a suitable driving signal has

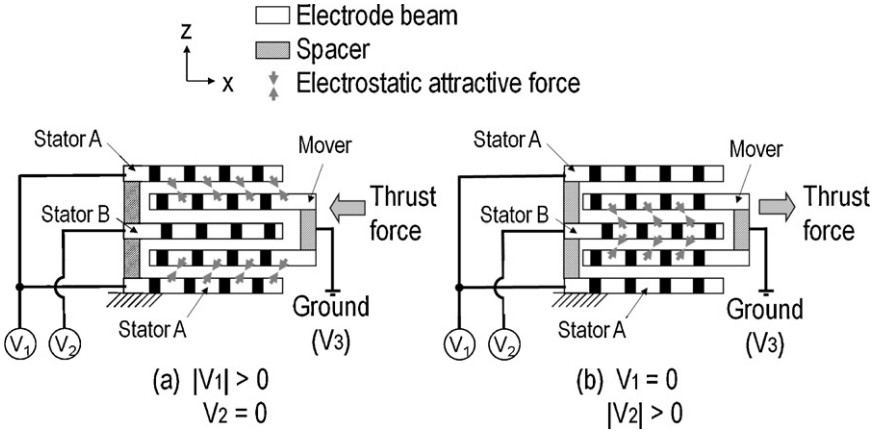

Fig. 2. Driving procedure for the bi-directional motion of the electrostatic actuator [36].

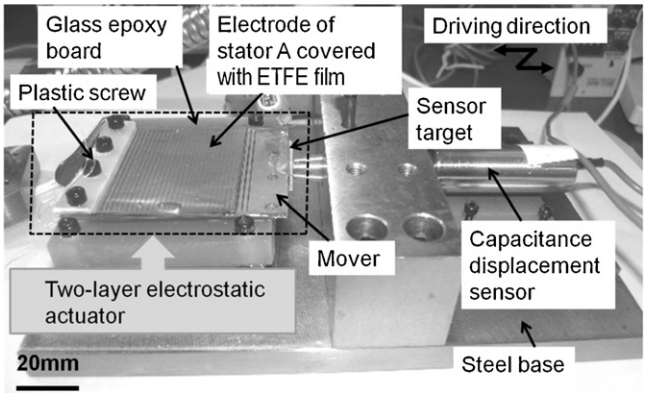

Fig. 3. Overview of the displacement measurement setup [36].

the potential to adjust the frictional effect for fine motion with a large holding force and a wide and fast motion. In the following section, the driving signal profiles for adjusting the frictional effect are discussed.

3.1. Effect of signal profile on displacement characteristics

The applied voltage between the electrode layers provides the charge to the electrode layers and the attractive force between them. The attractive force reduces the gap between the electrode layers and causes the mechanical contact between them. This behavior increases the frictional force. Typical control signals include direct current (DC) signals or component frequencies lower than the control bandwidth. In this paper, these signals are referred to as the normal signals. The normal signals generally apply voltage between the electrode layers long enough to gradually reduce the working range, as introduced in [36]. However, the normal signals do not make the working range zero. Fig. 4 shows the open-loop displacement characteristics for a periodic rectangular input signal after applying a constant voltage of 1 kV for 0.5 s. The displacement amplitude is much smaller than that without the applied voltage shown in [36]. The displacement amplitude gradually decreases. The experimental result suggests that the applied voltage generates the electric-charge leading to the mechanical contact and results in a large frictional force between the electrode layers. The large frictional force is useful as a holding force. On the other hand, the actuator produces displacement amplitude larger than 0.25 μm for 0.04 s after 0.5 s for a constant applied voltage of 1 kV. The change in the input signal quickly changes the displacement, which suggests that the working range is larger than the displacement amplitude. Hence, the normal signal is useful for adjusting fine motion with a large holding force, although the working range is limited. In this paper, the limited working range is referred to as the fine working range.

Table 1
Specifications of the electrostatic actuator.

Parameters	Value
Electrode width and length (mm)	50 × 50
Beam pitch (mm)	1.5
Spacer (mm)	50 × 6.5
Electrode thickness (mm)	0.1
Spacer thickness (mm)	0.4
ETFE film thickness (mm)	0.014
Electrode + ETFE film thickness (mm)	0.128
Thickness of assembled mover (mm)	0.656
Thickness of assembled stator (mm)	1.184
Gap between electrodes (mm)	0.244
Estimated silicon oil thickness (mm)	0.244
Mover mass (g)	5.22

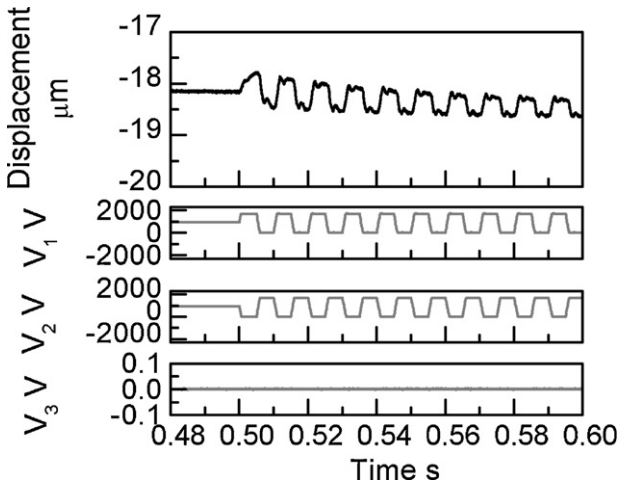

Fig. 4. Displacement response of the actuator to a normal signal with a 1 kV holding voltage using 10 mPas silicone oil.

In order to benefit from the large frictional force, the normal signal with a continuous constant voltage (referred to as the holding signal) is applied to the actuator. The aim of the holding signal is to assist in keeping the mover in the controlled position with added precision. In this paper, the combination of the normal signal and the holding signal is referred to as the fine driving mode signal, which is useful for the fine working range. Fig. 5 shows the relationship between the applied holding signals and the holding forces of the electrostatic actuator. The relationship was measured with a load cell. The symbols refer to the average data of three similar experiments. The curve represents the average approximate line calculated using the least-squares method based on Eq. (1). From this figure, it can be concluded that the increase in the holding voltage will affect the friction between the electrode layers due to the increased attractive forces between the electrode layers, which consequently generate a large holding force. It also can be seen that for a 1 kV holding signal, the actuator has a holding force of 0.205 N. At a 1 kV applied voltage, the estimated thrust force, which is calculated from the open-loop step displacement response based on the impulse signal as the wide driving signal [36], is 0.1896 N. Although this is lower than the measured holding force, the difference between the forces is not significant. The significant difference is that the use of the impulse signal shortens the period for generating the force. Additionally, the holding force is expected to be higher than the thrust force shown in [36] when the applied voltage is higher than 1.5 kV. In summary, the holding signal can adjust

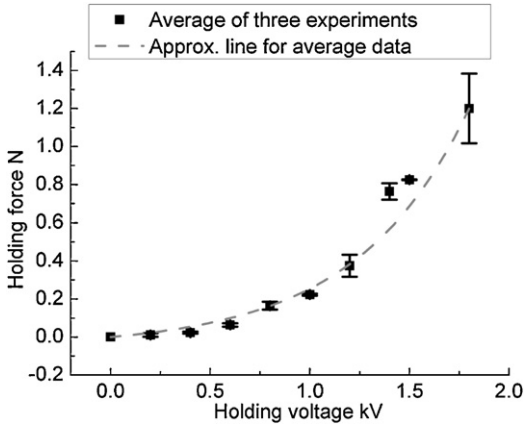

Fig. 5. Relationship between the applied holding signal and the holding force.

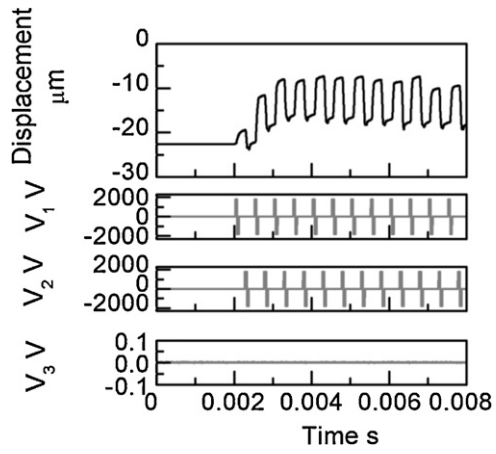

Fig. 6. Open-loop displacement characteristics using the impulse signal with a duty cycle of 1/5, a period of 0.5 ms and the 10 mPa·s silicone oil.

the frictional effect of the large holding force. In this study, 1 kV is selected as the evaluated holding signal.

$$F_{outputted} = k(V_{in}{}^2 - V_{\min}{}^2) \quad (1)$$

where $F_{outputted}$, outputted force by the actuator; k, force gain; V_{in}, applied voltage; V_{min}, minimum voltage to move the mover.

In order to avoid an increase in the frictional effect and also to ensure the full working range of the actuator, an impulse signal with a duty cycle of 1/5 has been proposed, as introduced in [36]. Fig. 6 shows the open-loop response of the mover to the impulse signal with a duty cycle of 1/5 using the 10 mPa s silicone oil. The impulse signal has a period of 0.5 ms. In this paper, the full working range is referred to as the wide working range. The impulse signal is used as the wide driving mode signal to ensure the full working range of the actuator [36]. The peak height for the wide driving mode signal is approximately 10 μm_{p-p}. As shown in Fig. 6, the displacement is shifted upward. The reason for this is considered to be that the frictional effect depends on the motion direction of the actuator. This signifies that the impulse signal does not reduce the working range and is useful for the wide working range.

3.2. Effect of holding signal

Fig. 7 shows the open-loop displacement characteristics using the fine driving mode signal comprising a square wave of 700 V and a holding signal of 1 kV. In Fig. 7(a), the actuator produces a displacement larger than 1.8 μm just after a period of 0.5 s for the holding voltage. After that, the amplitude of the reciprocating motion is kept at 0.15 μm for 0.6 s. And then the amplitude decreases again, but is kept at 0.07 μm after 6 s, as shown in Fig. 7(b). This suggests that the working range in the fine driving mode depends on the history of the input voltage, and the condition for switching between the two modes should be determined based on the desired motion. Similar to Fig. 6, it can be seen that the displacement is shifted upward. This also suggests that the frictional effect depends on the motion direction of the actuator. The fine motion with the holding force may cause the deformation of the insulation film which induces the displacement error in open-loop. However the error can be eliminated by feedback control.

As mentioned in Section 3.1, the applied voltage between the electrode layers increases the frictional force. This is because the attractive electrostatic force by the applied voltage causes the gap reduction between the electrode layers and makes the mechanical contact. For measuring the gap reduction between the electrode layers, the experimental setup shown in Fig. 8 was used. Fig. 9 shows the measured gap reduction between the electrode layers with respect to the holding signal. As shown in Fig. 8, the measured point was set roughly in the center of the actuator. The gap change tends to be influenced by the liquid. It can be seen that a 1 kV holding signal exhibits a gap reduction of 24 μm for a 0.5 s applied voltage period, and the waveform of the gap resembles first-order lag behavior. This is considered to result from the presence of the lubricating oil. The gap reduction indicates an increase in the frictional force, which acts as a large holding force. This lag behavior explains why the mover response for the fine driving mode signal in the traveling direction has a large amplitude that gradually decreases.

3.3. Improved signal for the full working range with a 1 kV holding signal

The electrostatic actuator supported by only lubricating oil can provide two driving modes, such as the fine and wide driving modes. In order to benefit from the two modes, rapid switching between the modes is desired. The active driving mode of the actuator influences the charge effect between the electrode layers generated by the driving signals. In the fine driving mode, a large charge effect plays an important role. The fine driving mode signal charges the insulation film and causes the mechanical contact, which is expected to increase the damping effect caused by the

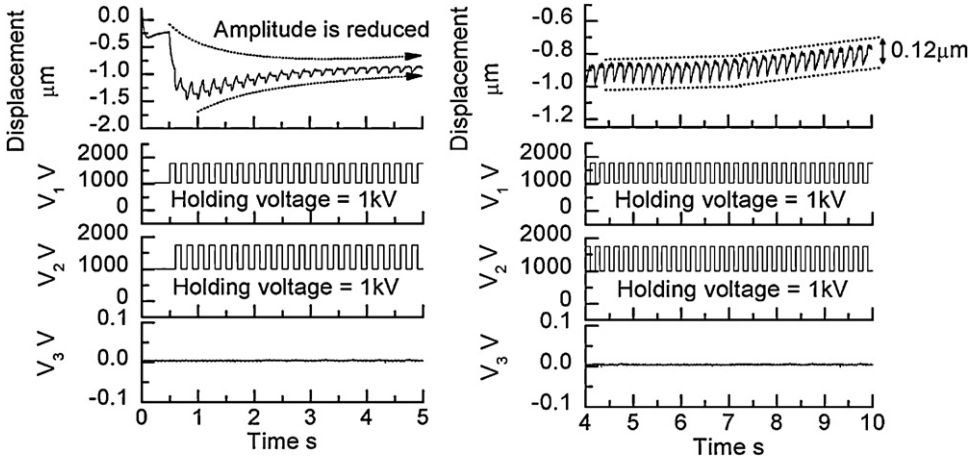

(a) Amplitude is reduced (b) Amplitude is maintained beyond 6 s

Fig. 7. Displacement characteristics under the fine driving mode signal.

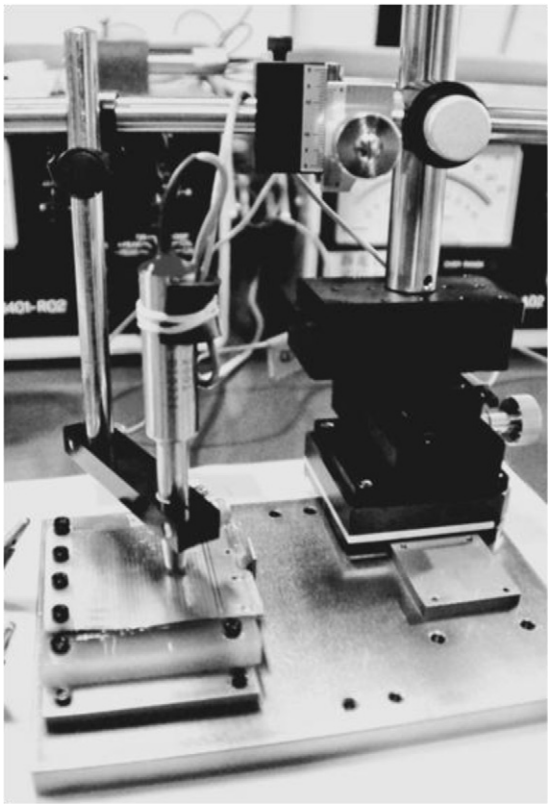

Fig. 8. Measurement setup for gap reduction measurement.

frictional force and decrease the residual vibration. In contrast, the charge effect generally can deteriorate the actuator characteristics in the wide driving mode.

Fig. 10 shows the displacement characteristics using the conventional wide driving mode signal shown in [36] after applying a 1 kV holding signal. It can be seen that the actuator does not show any significant displacement. This is because the large charge will remain in the electrode layers due to the 1 kV holding signal, and a large frictional force will be generated. Hence, a new wide driving mode signal that is less sensitive to the residual charge between the electrode layers after applying the 1 kV holding signal needs to be established.

Due to the insensitivity of the wide driving mode signal to the residual charge between the electrode layers from the 1 kV holding signal, an improved wide driving mode signal comprising a negative impulse signal is introduced. Fig. 11 shows the displacement characteristic using the improved wide driving mode signal after

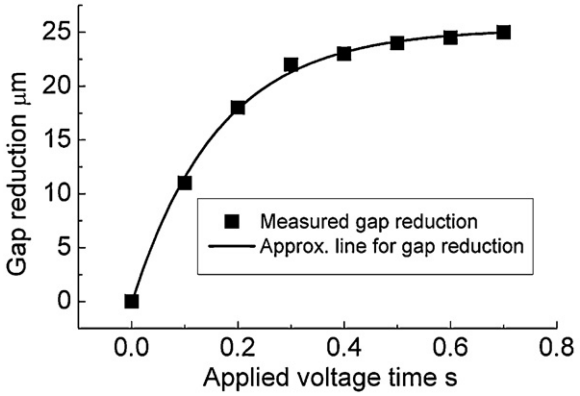

Fig. 9. Reduction in gap between electrodes from the 1 kV holding signal.

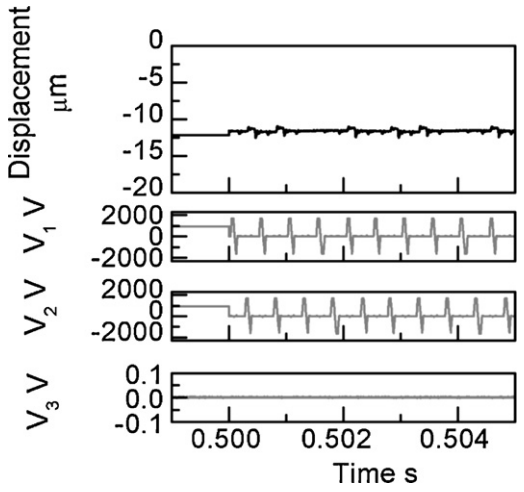

Fig. 10. Dual-motion displacement characteristics under the impulse signal after applying a 1 kV holding signal for 0.5 s with a 1.8 kV applied voltage.

applying the 1 kV holding signal. The peak height and period of the signal are 1.8 kV and 0.5 ms, respectively. It can be seen that the motions are kept at 10 μm_{p-p}. This indicates that the improved wide driving mode signal is less sensitive to the residual charge, hence enabling the actuator for a full working range of motion after applying the 1 kV holding signal. In the wide driving mode, the time for the applied voltage of 0 V is four times longer than the time for the high applied voltage. The time for 0 V is considered to work for the elimination of the residual charge caused by the high applied voltage. Fig. 12 summarizes the relationship between the amplitude of the applied negative impulse signal voltages with the 1 kV holding signal and the displacement characteristics. The symbols in Fig. 12 refer to the first amplitude of the displacement based on the negative impulse signals with different applied voltages. The time for the holding signal is fixed at 0.5 s. It can be seen that larger amplitudes of the negative impulse signal give larger displacements for both unidirectional motion and reciprocating motion. In addition, Fig. 12 shows that the displacement amplitudes for the unidirectional and reciprocating motions are somewhat similar under the same applied voltage. This indicates that the motion direction does not affect the displacement amplitude of the mover.

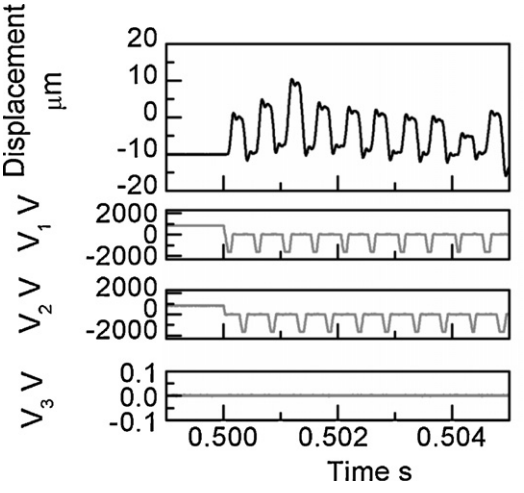

Fig. 11. Dual-motion displacement characteristics under the negative impulse signal after applying a 1 kV holding signal for 0.5 s with a 1.8 kV applied voltage.

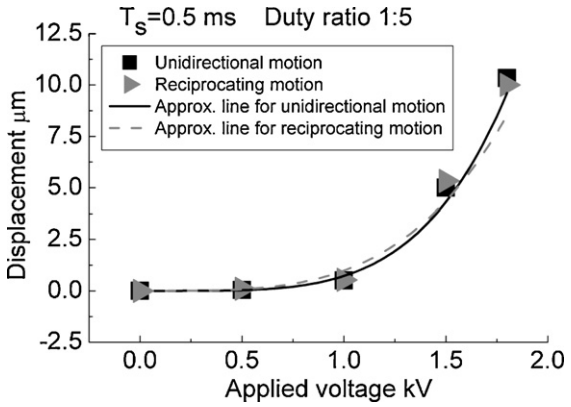

Fig. 12. Effects of applied negative impulse signal on the displacement with a 1 kV holding signal for 0.5 s.

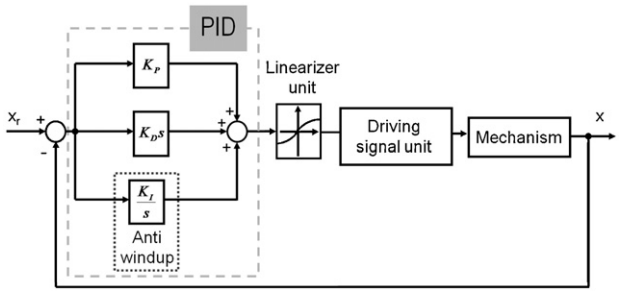

Fig. 13. Block diagram of the control system.

4. Control performance

4.1. Control system

In order to demonstrate the effectiveness of the characteristic switching function in a precision motion stage, a control system was designed based on a PID controller. Fig. 13 shows a block diagram of the control system. The control system includes the PID controller, a linearizer, and a driving signal unit. The linearizer is used to cancel the nonlinear characteristics between the input voltage and the thrust force. Fig. 14 shows the relationship between the applied negative impulse signal amplitude and the displacement from the signal. The output function of the linearizer is determined from the displacement characteristics shown in Fig. 14. The square symbols indicate the measured values. The solid line represents the approximate curve calculated from the data in Fig. 14 using the least-squares method. The driving signal unit is added to control the driving modes for characteristic switching based on the positioning error of the actuator. The control period is 0.5 ms, and the tuned PID controller parameters are $K_p = 25$, $K_i = 7.5$, and $K_d = 15$.

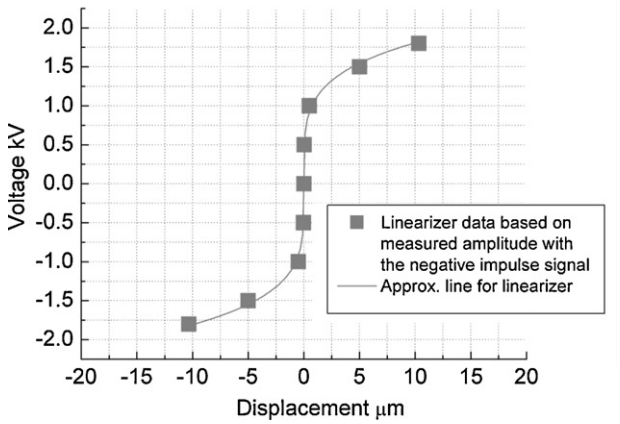

Fig. 14. Applied negative impulse signal to the displacement of the actuator with a 1 kV holding signal.

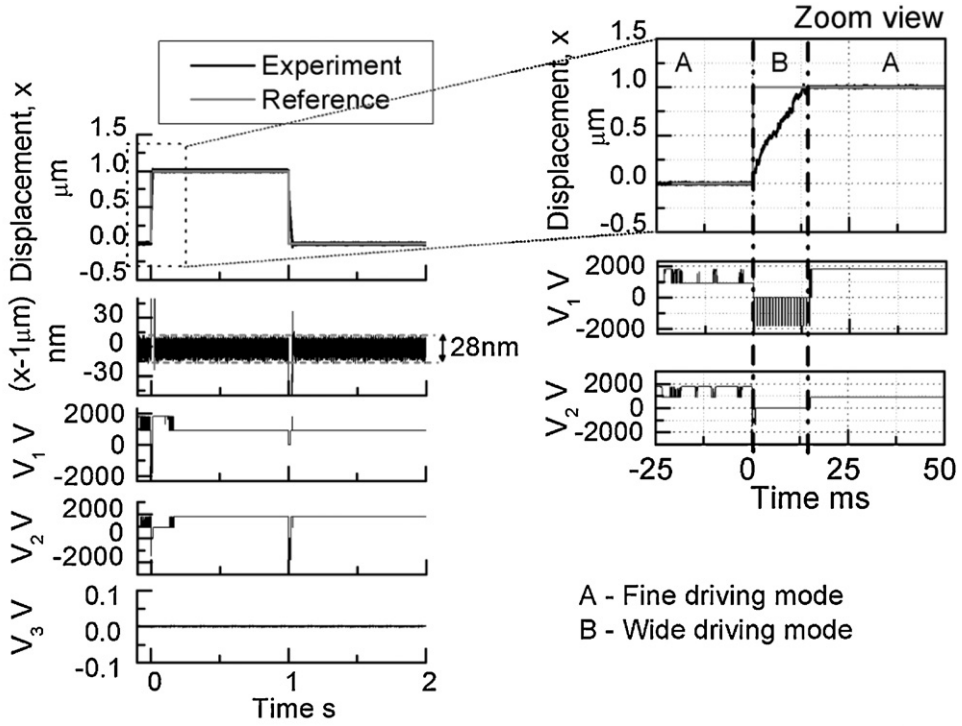

Fig. 15. Positioning performance using a 1 μm step input under the dual driving mode.

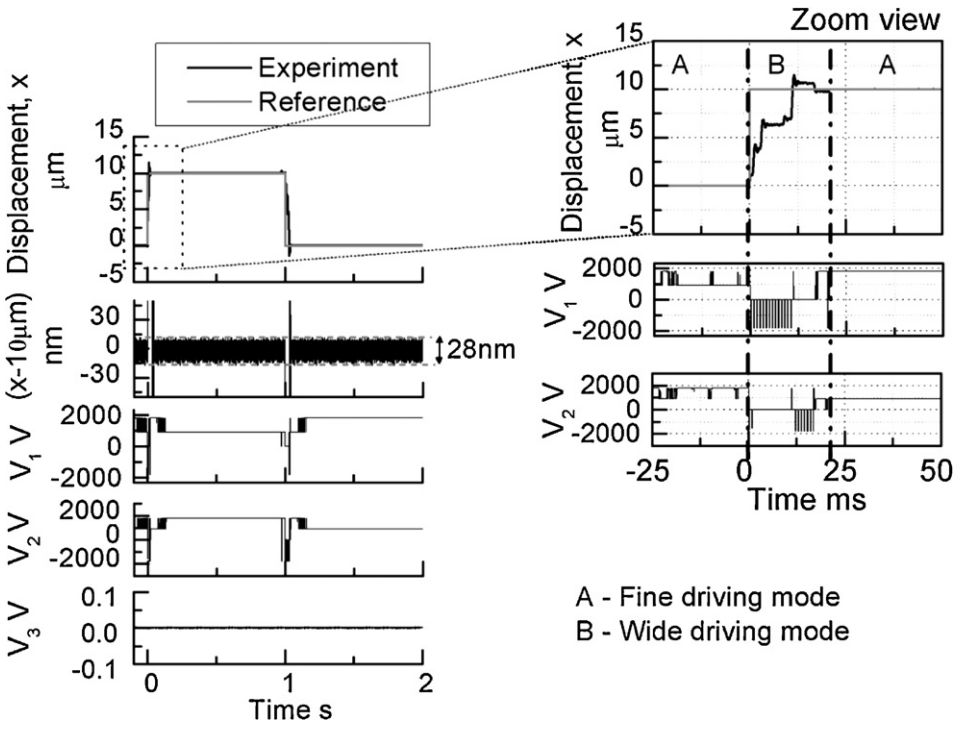

Fig. 16. Positioning performance using a 10 μm step input under the dual driving mode.

4.2. Experimental positioning and adjustment using the dual driving mode

To achieve the benefits of both the fine driving mode signal and the wide driving mode signal, a control method is devised. The combination of the wide driving mode and the fine driving mode is referred to as the dual driving mode. In the dual driving mode, the characteristic switching between the wide driving mode and the fine driving mode is carried out based on the positioning error of the actuator. As mentioned in Section 3.2, the working range of the fine driving mode is influenced by the input voltage history, and the condition for switching between the two modes should be determined based on the desired motion. In this section, the control system with the actuator is designed for PTP positioning, in which the two modes will be selected alternately. In this paper, the positioning error for switching between the two modes is determined to be 250 nm, which is smaller than the displacement amplitude just after the 0.5 s period for a holding voltage of 1 kV. The wide driving mode signal is comprised of a negative impulse signal with a 0.5 ms control period. When the positioning error is larger than 250 nm, the wide driving mode signal is applied for a small charge effect. Then, when the positioning error is smaller than or equal to 250 nm,

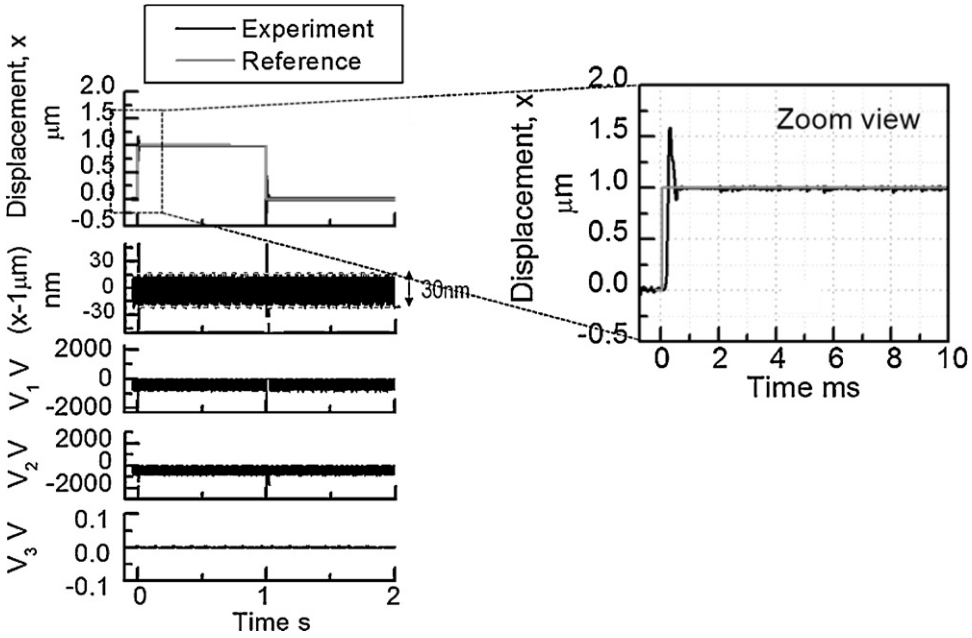

Fig. 17. Positioning performance using a 1 μm step input under the wide driving mode.

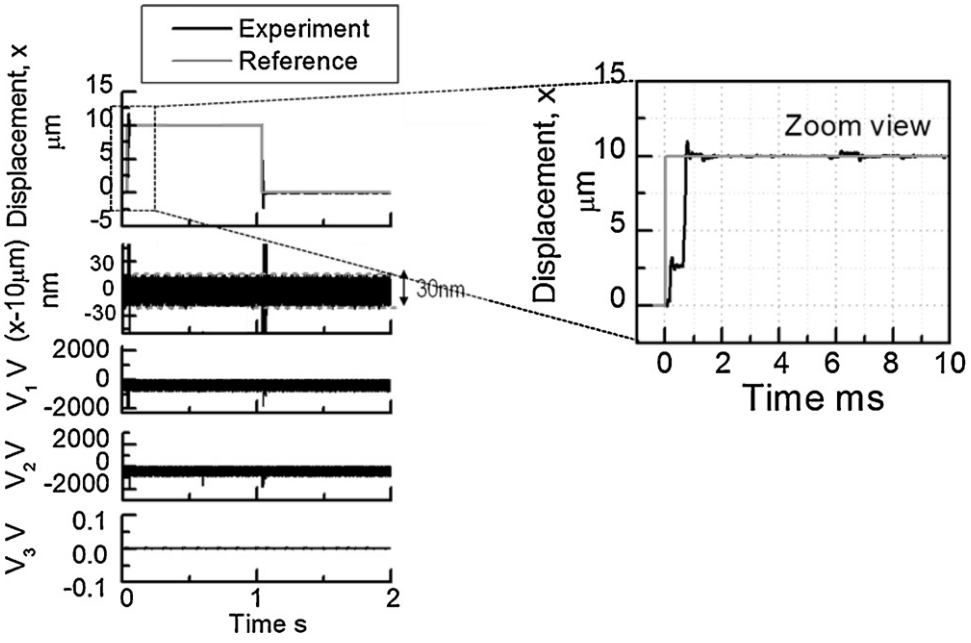

Fig. 18. Positioning performance using a 10 μm step input under the wide driving mode.

the fine driving mode signal is applied. The fine driving mode signal comprises a normal signal and a 1 kV holding signal. The attractive force generated by the holding signal makes the contact between the electrode layers and provides a large frictional force. The large frictional force in the fine driving mode is expected to improve the damping characteristic and helps to reduce the overshoot and residual vibration.

The positioning performance based on the characteristic switching between the wide driving mode and the fine driving mode is evaluated experimentally. As discussed in Section 3, the motion

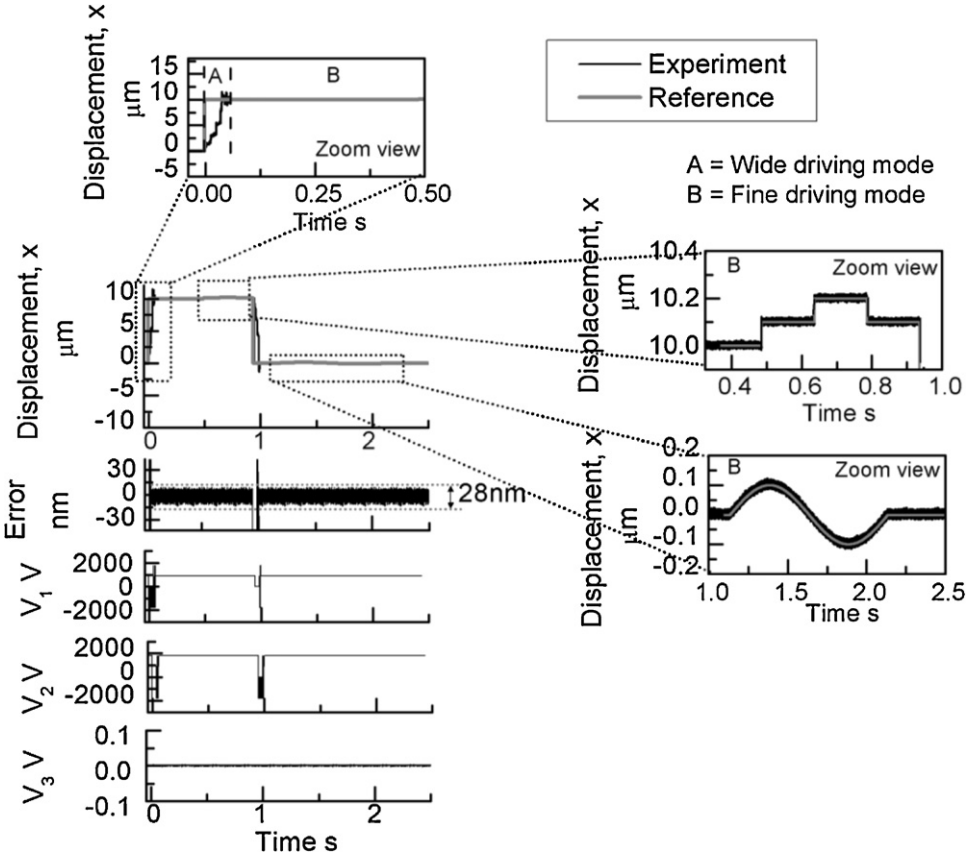

Fig. 19. Positioning performance using a mixed input reference (step, stepwise, and sinusoidal input) under the dual driving mode.

characteristics of the actuator are greatly influenced by the profile of the input signal due to the friction between the electrode layers. Figs. 15 and 16 show the positioning results of the dual driving mode using step inputs of 1 μm and 10 μm, respectively. The negative impulse signal is applied in a short period for the wide driving mode (the B period in Figs. 15 and 16). And then the normal signal and the holding signal is applied for the fine driving mode (the A period). The positioning errors are smaller than 14 nm and those under the wide driving mode shown in Figs. 17 and 18. Also, it can be seen that the average percent overshoot for a step height of 1 μm using the dual driving mode is reduced to 3.55% compared with 57.70% for the wide driving mode (based on 10 identical experiments). For a step height of 10 μm, the percentage overshoot is reduced to 13.74% compared with 31.58% for the wide driving mode. The reduction of the steady state positioning error and the overshoot shows the usefulness of the improved damping characteristics caused by the frictional force.

The dual driving mode used in Figs. 15 and 16 exhibits a longer rise time for both step heights compared with the wide driving mode used in Figs. 17 and 18; this suggests that the gap is still not restored enough which gives a small damping effect. However, the mover is positioned precisely and the residual vibrations in the dual driving mode are lower than those in the wide driving mode. In total, the dual driving mode exhibits a better transient response in terms of the residual vibration and the percentage overshoot. This feature looks like control systems with a high differential gain element. However the advantage of the dual driving mode is to provide a continuous holding force without a feedback element.

Fig. 19 demonstrates the combination of wide step responses and fine motion adjustments in the dual driving mode. The input signal consists of a step height input of 10 μm, a 0.1 μm stepwise input with a 0.15 s interval time, and a 0.1 μm sinusoidal input. The positioning error in the fine driving mode is smaller than 14 nm. This result demonstrates the high positioning performance and high adjustment performance near the reference position under the dual driving mode.

5. Conclusions

In summary, this paper focused on the characteristic switching of a multilayer thin electrostatic actuator supported by only lubricating oil, which enables a large holding force. Its characteristics, such as the working range and the frictional force (which is useful as a holding force between electrode layers), are significantly affected by the applied driving signal. The characteristic switching is useful for the control of a precision positioning stage. Thus, the relationships between the characteristics and the driving signals have been examined in detail. The open-loop experimental results show that the two driving modes (i.e., the fine driving mode for fine motion with a continuous holding force and the wide driving mode for the full working range of motion) can be derived and switched using suitable driving signals. Then, a control system with a multilayer electrostatic actuator was designed using the dual driving mode, which integrates the wide and fine driving modes. The positioning performance was then evaluated. It was proven that the control system using the dual driving mode has a positioning error smaller than 14 nm and provides a continuous holding force, although the rise time was elongated. The positioning errors and the overshoots for the dual driving mode were also smaller than those for just the wide driving mode. Furthermore, the combinations of PTP positioning and ultra-precision position adjustment with a large holding force near the reference position were demonstrated. These prove the usefulness of characteristic switching of the multilayer electrostatic actuator supported by only lubricating oil.

References

[1] Ando Y. Development of three-dimensional electrostatic stages for scanning probe microscope. Sensors and Actuators A 2004;114:285–91.
[2] Binning G, Rohrer H, Gerber C, Weibel E. Surface studies by scanning tunneling microscopy. Physical Review Letters 1982;49(1):57–60.
[3] Uchihashi T, Sugawara Y, Tsukamoto T, Ohta M, Morita S. Role of a covalent bonding interaction in noncontact-mode atomic-force microscopy on Si(1 1 1)7 × 7. Physical Reviews B 1997;56(15):9834–40.
[4] Rudnitsky RG, Chow EM, Kenny TW. Rapid biochemical detection and differentiation with magnetic force microscope cantilever arrays. Sensors and Actuators 2000;83:256–62.
[5] Ando Y, Ino J. Friction and pull-off forces on submicron-size asperities. Wear 1998;216:115–22.
[6] Lim MG, Muller RS, Kim CJ, Pisano AP. Polysilicon microgripper. Sensors and Actuators A 1992;33:221.
[7] Diem B, Rey P, Renard S, Bosson SV, Bono H, Michel F, et al. SOI 'SIMOX': from bulk to surface micromachining, a new age for silicon sensors and actuators. Sensors and Actuators A 1995;46–47:8–16.
[8] Lee D, Krishnamoorthy U, Yu K, Solgaard O. High-resolution, high-speed microscanner in single-crystalline silicon actuated by self-aligned dual-mode vertical electrostatic comb drive with capability for phased array operation. Transducers, Solid-State Sensors, Actuators and Microsystems 2003: 576–9.
[9] Ando Y, Ikehara T, Matsumoto S. Design, fabrication and testing of new comb actuators realizing three-dimensional continuous motions. Sensors and Actuators A 2002;9:7–98, 579–586.
[10] Wu WG, Li DC, Suna W, Hao YL, Yan GZ, Jin SJ. Fabrication and characterization of torsion-mirror actuators for optical networking applications. Sensors and Actuators A 2003;108:175–81.
[11] Guerre R, Hibert C, Burri Y, Flückiger PH, Renaud PH. Fabrication of vertical digital silicon optical micro mirrors on suspended electrode for guided-wave optical switching applications. Sensors and Actuators A 2005;123–124: 570–83.
[12] Mineta T, Kida N, Nomura S, Makino E. Pulsation sensor integrated with micro vascular holding actuator for thrombosis monitoring. Sensors and Actuators A 2008;143:14–9.
[13] Jang SL, Li SH, Lin LS. Silicon controlled rectifiers type electrostatic discharge protection circuits with variable holding voltage. Solid-State Electronics 2001;45:689–96.
[14] Kang M, Song KW, Park BG, Shin H. The novel SCR-based ESD protection with low triggering and high holding voltages. Microelectronics Journal 2011;42:837–9.
[15] Guo ZJ, McGruer NE, Adams GG. Modeling, simulation and measurement of the dynamic performance of an ohmic contact, electrostatically actuated RF MEMS switch. Journal of Micromechanics and Microengineering 2007;17:1899–909.
[16] Tsou CC, Lin WT, Fan CC, Chou CS. A novel self-aligned vertical electrostatic comb drives actuator for scanning micromirrors. Journal of Micromechanics and Microengineering 2005;15:855–60.
[17] Strandman C, Bäcklund Y. Bulk silicon holding structures for mounting of optical fibers in V-grooves. Journal of Microelectromechanical Systems 1997;6(1):35–40.
[18] Hwang IH, Lee YG, Lee JH. A micromachined friction meter for silicon sidewalls with consideration of contact surface shape. Journal of Micromechanics and Microengineering 2006;16:2475–81.
[19] Liu YT, Wang CW. A self-moving precision positioning stage utilizing impact force of spring-mounted piezoelectric actuator. Sensors and Actuators A 2002;102:83–92.
[20] Chen SJS, Vishniac IJB. A magnetically levitated, automated, contact analytical probe tool. IEEE Transactions on Semiconductor Manufacturing 1995;8:72–8.
[21] Chan KW, Liao WH, Shen IY. Precision positioning of hard disk drives using piezoelectric actuators with passive damping. IEEE/ASM. Transactions on Mechatronics 2008;13(1):147–51.
[22] Cueff M, Defaÿ E, Rey P, Le Rhun G, Perruchot F, Ferrandon C, et al. A fully packaged piezoelectric switch with low voltage actuation and electrostatic hold. In: IEEE 23rd International Conference on Micro Electro Mechanical Systems (MEMS). 2010. p. 212–5.
[23] Lin W, Ann NK, Ng LE. Concepts for a class of novel piezoelectric self-locking long-stroke actuators. Precision Engineering 2002;26:141–54.
[24] Cueff M, Defaÿ E, Le Rhun G, Rey P, Perruchot F, Suhm A, et al. Integrated metallic gauge in a piezoelectric cantilever. Sensors and Actuators A: Physical 2011;5:1027–30.
[25] Hii KF, Vallancea RR, Mengüc MP. Design, operation, and motion characteristics of a precise piezoelectric linear motor. Precision Engineering 2010;34:231–41.
[26] Petit L, Prelle C, Dore E, Lamarque F, Bigerelle M. A four-discrete-position electromagnetic actuator: modeling and experimentation. IEEE/ASM. Transactions on Mechatronics 2010;15(1):88–96.
[27] Kube H, Zoeppig V, Hermann R, Hoffmann A, Kallenbach E. Electromagnetic miniactuators using thin magnetic layers. Smart Material and Structures 2000;9:334–6.
[28] Kim WJ, Verma S, Shakir H. Design and precision construction of novel magnetic-levitation-based multi-axis nanoscale positioning systems. Precision Engineering 2007;31:337–50.
[29] Kuo SK, Menq CH. Modeling and control of a six-axis precision motion control stage. IEEE/ASM. Transactions on Mechatronics 2005;10(1):50–9.

[30] Ludwick SJ, Trumper DL, Holmes ML. Modeling and control of a six degree-of-freedom magnetic fluidic motion control stage. IEEE Transactions on Control Systems Technology 1996;4(5):553–64.
[31] Niino T, Egawa S, Higuchi T. Dual excitation multiphase electrostatic drive. In: Proceeding of the Industry Application Society Annual Meeting. 1995. p. 1318–25.
[32] Yamamoto A, Niino T, Higuchi T. Modeling and identification of an electrostatic motor. Precision Engineering 2006;30:104–13.
[33] Modafe A, Ghalichechian N, Frey A, Lang JH, Ghodssi R. Microball-bearing-supported electrostatic micromachines with polymer dielectric films for elecromechanical power conversion. Journal of Micromechanics and Microengineering 2006;16:182–90.
[34] Beyaz MI, Carthy MM, Ghalichechian N, Ghodssi R. Closed-loop control of long-range micropositioner using integrated photodiode sensors. Sensors and Actuators A 2009:187–94.
[35] Yamashita N, Zhang ZG, Yamamoto A, Gondo M, Higuchi T. Voltage-induction type electrostatic film motor driven by two- to four-phase ac voltage and electrostatic induction. Sensors and Actuators A 2007;140:239–50.
[36] Mariam MG, Sato K. Basic characteristics of a multilayer electrostatic actuator supported by lubricating oil for a fine-motion stage. Precision Engineering 2012;36:77–83.